Journal of Alloys and Compounds 543 (2012) 159–166

Contents lists available at SciVerse ScienceDirect

Journal of Alloys and Compounds

journal homepage: www.elsevier.com/locate/jalcom

Optimizing preparation of carbon supported cobalt catalyst for hydrogen generation from $NaBH_4$ hydrolysis

Weiling Niu [a], Dengbo Ren [b], Yuanyuan Han [a], Yanjun Wu [a], Xinglong Gou [a,*]

[a] Chemical Synthesis and Pollution Control Key Laboratory of Sichuan Province, College of Chemistry and Chemical Engineering, China West Normal University, Nanchong 637000, PR China

[b] Division of Academic Affairs, Sichuan University of Arts and Science, Dazhou 635000, PR China

ARTICLE INFO

Article history:
Received 9 April 2012
Received in revised form 12 July 2012
Accepted 14 July 2012
Available online 31 July 2012

Keywords:
Hydrogen generation
Sodium borohydride
Hydrolysis
Cobalt catalyst
Ball-milling
Kinetics

ABSTRACT

Modified carbon-supported cobalt catalysts have been synthesized by optimization of the preparation conditions including ball-milling pretreatment of the carbon and screening the solvents used for synthesis of the catalysts. Ball-milling treatment on carbon can not only reduce its particle size but also functionalize the surface with oxygen-containing groups, resulting in good affinity to Co^{2+} ions. The non-aqueous solvent *N*,*N*-dimethylformamide (DMF) is beneficial to improve the immersional wetting and adsorption of the cobalt salt solution on the surface of carbon, leading to uniform deposition of cobalt nanoparticles upon chemical reduction. The carbon-supported cobalt catalyst with the Co loading of 13.20 wt% obtained under optimum conditions exhibits excellent catalytic activity toward $NaBH_4$ hydrolysis and the average hydrogen generation rate at 27 °C is 10.29 L_{H_2} min^{-1} $g^{-1}_{(cobalt)}$ corresponding to a turnover frequency of 1473.4 mol H_2 (mol cobalt)$^{-1}$ h^{-1}, which is higher than the most reported data. Furthermore, the effects of the cobalt loading, catalyst dosage, concentration of NaOH and $NaBH_4$, and reaction temperature on the hydrogen generation have been investigated by hydrolysis of alkaline $NaBH_4$ solution, and the corresponding rate equation can be described as $r = A\exp(-42190/RT)[\text{cobalt}]^{0.16}[\text{NaOH}]^{0.23}[\text{NaBH}_4]^{0.30}$.

1. Introduction

Hydrogen is a clean and green fuel with little or nor harmful emissions, and is now widely recognized as an attractive alternative to fossil fuels, capable of providing energy security and sustainability, along with environmental and socioeconomic benefits [1]. However, efficient hydrogen generation and storage still remain a great challenge for its large scale applications [2–5].

Recently, sodium borohydride ($NaBH_4$) has gained increasing attention as a promising source to supply hydrogen for proton exchange membrane fuel cells due to its combined advantages of high hydrogen content (10.8 wt%), nontoxicity, and excellent stability of its alkaline solution [6–9]. Moreover, high purity of hydrogen can be controllably generated on demand by catalytic hydrolysis of $NaBH_4$ in the presence of appropriate catalyst [10]. Therefore, development of effective catalysts for $NaBH_4$ hydrolysis is of great scientific and technological importance.

During the past decades a variety of catalysts including precious metals and non-noble metals (usually functionalized with a support) have been developed for hydrogen generation from $NaBH_4$ hydrolysis [11–14]. Among the investigated catalysts, carbon-supported cobalt metals or alloys are proven to be efficient catalysts with the advantages of low cost and high catalytic activity [15]. Generally, the carbon-supported Co catalysts are prepared by impregnation of carbon powders into an aqueous $CoCl_2$ solution followed by chemical reduction. It is also found that the catalytic activity of the catalysts is sensitive to their preparation conditions. Kim et al. investigated the effects of different precursors ($CoCl_2$ and $CoSO_4$), $NaBH_4/Co^{2+}$ mole ratios (0.67–3) and calcination temperatures (130–450 °C) on the properties of the prepared Co–B catalyst, and found that a maximum hydrogen generation rate (HGR) of 2.4 L min^{-1} g^{-1}_{cat} can be obtained only under the optimum conditions with $CoCl_2$ as the precursor, a $NaBH_4/Co^{2+}$ mole ratio of 1.5 and calcination at 250 °C [16]. Liu et al. found that the catalytic properties of the Co–B catalysts were sensitive to the pH value of the $NaBH_4$ reduction solution and mixing manner of the precursors [17]. To further improve the performance of cobalt-based catalysts some measurements have been taken to control the cobalt dispersion and modify the surface chemistry of the carbon used. For example, Chen et al. employed ethylenediamine as a complex agent for Co^{2+} ions to improve the dispersion of Co–B particles on the surface of the carbon, and achieved a maximum HGR of 2.07 L_{H_2} min^{-1} g^{-1}_{cat} [18]. Shen et al. used oxygen-containing groups functionalized multiwalled carbon nanotubes (MWCNTs) as the support of Co–B catalysts, resulting in a HGR of 5.1 L_{H_2} min^{-1} g^{-1}_{cat} [19]. Patel et al. prepared Co–B nanoparticles supported on carbon film catalyst by pulsed laser deposition technique to improve the

* Corresponding author. Tel.: +86 817 256 8081; fax: +86 817 256 8081.
E-mail address: gouxlr@126.com (X. Gou).

0925-8388/$ - see front matter © 2012 Elsevier B.V. All rights reserved.
http://dx.doi.org/10.1016/j.jallcom.2012.07.099

specific surface area of both the carbon support and Co–B nanoparticles, and obtain a high HGR of 8.1 L_{H_2} min^{-1} g_{cat}^{-1} in the hydrolysis of $NaBH_4$ [20]. Although great progresses have been made in the field of hydrogen generation from $NaBH_4$ hydrolysis catalyzed by carbon-supported cobalt catalysts, facile methods for preparing the needed catalysts with excellent activity are still highly desired.

In this paper, influences of some preparation parameters such as mechanical milling pretreatment of the carbon support under aerobic/anaerobic conditions and the solvents (de-ionized water, absolute ethanol, and DMF) used for preparation of the catalyst on its catalytic activity toward hydrolysis of sodium borohydride have been investigated, and an average HGR of 10.29 L_{H_2} min^{-1} $g_{(cobalt)}^{-1}$, corresponding to a turnover frequency (TOF) of 1473.4 mol H_2 (mol cobalt)$^{-1}$ h^{-1}, was achieved at 27 °C by using the optimized carbon-supported Co catalysts.

2. Experimental

2.1. Catalyst preparation

All chemicals including $CoCl_2 \cdot 6H_2O$, $NaBH_4$, NaOH, ethanol, and dimethylformamide (DMF) are of analytical grade. Commercial cylindrical activated carbon was used as a typical carbon support. It was first manually ground into powder, and then partial of the powder was further mechanically milled under aerobic or anaerobic conditions using a planetary high-energy ball mill (model QM-3SP2, Nanjing NanDa Instrument Plant) with different weight ratio of ball to carbon (10:1–20:1), rotation speeds (350–550 rpm), and milling time (5–15 h) to investigate the effect of milling pretreatment on the catalytic activity of the carbon-supported cobalt catalysts.

The carbon-supported cobalt catalysts were prepared by a modified impregnation-chemical reduction method, in which DMF, absolute ethanol as well as de-ionized water (DW) was respectively used as the solvent for dissolving both cobalt salt and $NaBH_4$ to investigate the solvent effect. In a typical procedure, 0.5 g carbon powder (hand-grinded or milled ones under different conditions) was first dispersed into 10 mL $CoCl_2$ solution (0.14 mol L^{-1}) with the help of ultrasonication, and then the mixture was stirred overnight to reach adsorption equilibrium. Subsequently, freshly prepared $NaBH_4$ solution (10 mL, 0.56 mol L^{-1}) with the same solvent as the $CoCl_2$-carbon dispersion was added dropwise under continuous stirring. Finally, the resulting black precipitates were collected by centrifugation, washed and dried in vacuum at 60 °C for 24 h. By adjusting the initial ratio of carbon to Co^{2+}, a series of catalysts with different Co loading (13.20, 17.48, and 19.34 wt%) were obtained.

2.2. Catalyst characterization

The chemical composition of the samples was characterized by X-ray diffraction (XRD, Rigaku Ultima IV, Cu Kα radiation). The morphology of the catalysts was observed by scanning electron microscope (SEM, JEOL JSM-6510LV) coupled with an energy-dispersive X-ray spectroscopy (EDS, Oxford instruments X-Max). The cobalt loading of the supported catalyst as well as the elemental distribution on the carbon support was determined by EDS analysis, and an average value of six different areas was reported for each sample (the standard derivation was less than 0.3%). Transmission electron microscope (TEM) images were taken using a FEI Tecnai G20 microscope operated at 200 kV. The specific surface area of the sample was measured by Brunauer–Emmett–Teller (BET) nitrogen adsorption–desorption method on a Belsorp-Mini II instrument (BEL Japan, Inc.). Fourier transform infrared spectroscopy (FTIR) was recorded on Thermo Sientific Nicolet 6700 FT-IR spectrometer.

2.3. Hydrogen generation measurements

Catalytic activity of the as-prepared catalysts for hydrogen generation from the hydrolysis of alkaline $NaBH_4$ solution was evaluated in a batch reactor. In a typical experiment, an appropriate amount of the catalyst was first loaded into a 50 mL round-bottom flask, which was immersed in a thermostatic water bath to keep the temperature constant. Then, 10 mL of aqueous solution containing $NaBH_4$ and NaOH with a given concentration was quickly added into the flask under stirring to initiate the hydrolysis reaction. The volume of the hydrogen evolved was measured by a classic water-displacement method and was transformed to the value in standard temperature and pressure. The hydrogen generation rate (HGR) was normalized by per unit weight of the active cobalt catalyst and was defined as L_{H_2} min^{-1} $g_{(cobalt)}^{-1}$.

3. Results and discussion

3.1. Optimizing the preparation conditions of carbon-supported cobalt catalyst

$NaBH_4$ hydrolysis catalyzed by a carbon-supported catalyst is a heterogeneous reaction, and thus the HGR strongly depends on the surface properties of the catalyst, which is directly related to the preparation conditions. The purpose of this work is to investigate the potential effects of both the pretreatment of carbon support with ball milling and the solvents used for preparation of the composite catalyst on the hydrogen generation activity of the prepared catalyst.

3.1.1. Effect of ball-milling pretreatment of the carbon support

High-energy ball milling is reported to be an efficient mechanochemical technique to reduce the particle size and enhance the surface properties of the studied materials [21–23]. Herein, milling technique is employed to improve the surface activity of the carbon support, and the effects of milling parameters on the catalytic activity of the supported catalyst were evaluated by the average HGR for catalytic hydrolysis of 1 wt% $NaBH_4$ solution containing 8 wt% NaOH at 27 °C in the presence of 20 mg the carbon-supported cobalt nanoparticles with a Co loading of 13.20 wt%.

Fig. 1(a) shows the effect of the ball-to-carbon weight ratio on the HGR for the carbon-supported cobalt catalysts. Obviously, the ball-milled carbon supported cobalt catalysts always exhibit much higher HGR than the one using the hand-ground carbon as the support. Moreover, the HGR improved markedly when the ball-to-carbon weight ratio increased from 10:1 to 15:1, and an average HGR of 10.23 L min^{-1} g^{-1} was achieved at this point, which is almost 4 times higher than that for the hand-ground carbon supported catalyst. It was also observed that further increase in the ball-to-carbon weight ratio had little effect on the HGR. Therefore, the optimum ball-to-carbon weight ratio was selected as 15:1 in this work.

From the inset of Fig. 1(b) we can see that the milling speed has an important effect on the HGR. Especially, a sharp increase in HGR is observed when the milling speed rises from 350 to 450 rpm. Afterwards, the HGR increases only slightly when the milling speed rises from 450 to 550 rpm. This trend is consistent with the order of the BET specific surface area, which is 405.4, 429.5 and 430.7 m^2 g^{-1} for the milled carbon obtained at 350, 450 and 550 rpm, respectively. Therefore, the optimum milling speed was chosen as 450 rpm to further investigate the influence of the milling time on HGR, and the result is presented in Fig. 1(b). With the milling time changing from 5 to 10 h, an evident increase in the HGR is observed from 9.69 to 10.29 L_{H_2} min^{-1} g^{-1}. Thereafter, a very gentle change in HGR occurs with continuous increase of

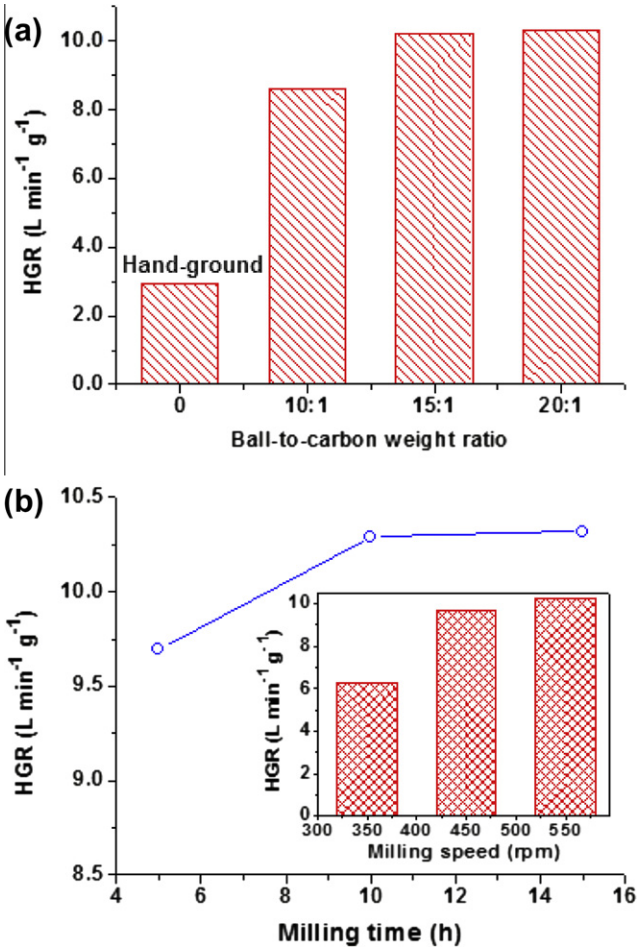

Fig. 1. Effects of milling conditions on the hydrogen generation activity of the carbon-supported cobalt catalysts (20 mg, the Co loading is 13.20 wt%) by catalytic hydrolysis of 1 wt% $NaBH_4$ solution containing 8 wt% NaOH at 27 °C. (a) Influence of the ball-to-carbon weight ratio on the HGR, where the milling time and speed was set as 5 h and 550 rpm, respectively. (b) Influence of milling time on the HGR at a milling speed of 450 rpm. The inset is the influence of milling speed on the HGR, where the milling time was set as 5 h.

the milling time. Accordingly, 10 h is sufficient for the ball milling treatment of the carbon support.

FTIR spectrum can reveals the details about the surface chemical composition of a material. For the sake of comparison Fig. 2 presents the FTIR spectra of the hand-ground carbon, and the ball-milled ones under both anaerobic and aerobic conditions. Overall, all the studied carbon samples exhibits three pronounced bands at 1137, 1582, and 3450 cm^{-1}, respectively. The broad peak near 1137 cm^{-1} is a superposition of a number of overlapping bands of ether, epoxide, lactone and phenolic structures in different environments [24]. The peak at 1582 cm^{-1} is a characteristic peak for carbon materials containing aromatic rings or ether-like bonds [25]. The broad peak around 3450 cm^{-1} can be assigned to O–H stretching vibrations of surface hydroxylic groups and chemisorbed water [25]. However, the intensity of the peaks related to the oxygen-containing groups in the spectrum of the carbon milled in air increases significantly, indicating that the high energy provided by ball milling exacerbates the oxidization of carbon in air, and thus produces a large quantity of oxygen-containing groups on its surface. In contrast, the oxidization of carbon is heavily inhibited in the ball-milling process without air, or it is negligible during the hand-ground treatment in air due to lack of enough energy. As a support for catalyst the oxygen-rich functional groups on the ball-milled carbon exhibits enhanced affinity to metal ions,

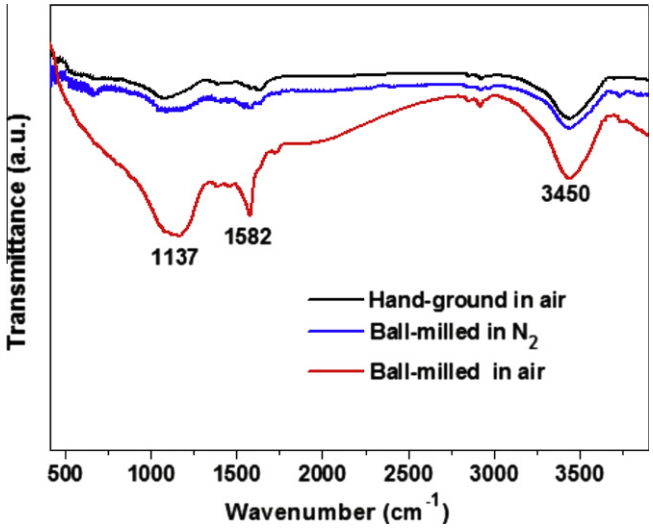

Fig. 2. FTIR spectra of the hand-ground carbon and the ball-milled ones obtained under anaerobic and aerobic conditions.

resulting in good dispersion of the chemically reduced metal nanoparticles on its surface and high catalytic activity for hydrolysis of $NaBH_4$.

The above experiments suggest that ball-milling treatment on carbon in air can improve its surface area and chemical composition, leading to an improvement of the catalytic hydrogen generation activity of cobalt nanoparticles supported on it in the hydrolysis of sodium borohydride. The optimum milling conditions were found to be 15:1 for the ball-to-carbon weight ratio, 450 rpm for the milling speed, and 10 h for the milling time.

3.1.2. Effect of the solvents used for preparation of the catalyst

Carbon-supported cobalt catalyst is usually prepared by an impregnation-chemical reduction method in the literatures, where de-ionized water (DW) is often used as the solvent to dissolve cobalt salt and also as the disperse media for carbon support. However, the hydrophobic characteristic of the carbon support might restrict effective contact between the carbon surface and the aqueous Co^{2+} solution, and thus would affect the deposition and dispersion of the cobalt metals in the course of chemical reduction process. We surmise that the catalytic performance of the carbon-supported cobalt catalysts can also be improved by selecting an appropriate solvent, which not only dissolve the cobalt salt but also infiltrate the surface and pore of the carbon support. Based on this consideration, we prepared three kinds of carbon-supported cobalt catalysts by respectively using DW, absolute ethanol and DMF as the solvent and disperse media. Fig. 3 displays the HGR over the three kinds of catalysts under the same hydrolysis conditions. As expected, the corresponding HGR at 27 °C increases from 2.41, 6.64 to 10.29 L_{H_2} min^{-1} g^{-1}, corresponding to a turnover frequency of 345.06, 950.71 and 1473.4 mol H_2 (mol Co)$^{-1}$ h^{-1}, respectively. Therefore, DMF is the best solvent for preparation of the carbon-supported cobalt catalysts.

3.2. Chemical composition and structure of the catalyst

Fig. 4 presents the XRD patterns of the unsupported cobalt particles (a), the carbon support after ball-milling treatment (b), and the carbon-supported Co catalyst prepared under the optimum conditions (c). Fig. 4(a) indicates that the unsupported cobalt particles are partially oxidized into cobalt oxides. Similar phenomenon is often observed for the cobalt-based catalysts [26]. By

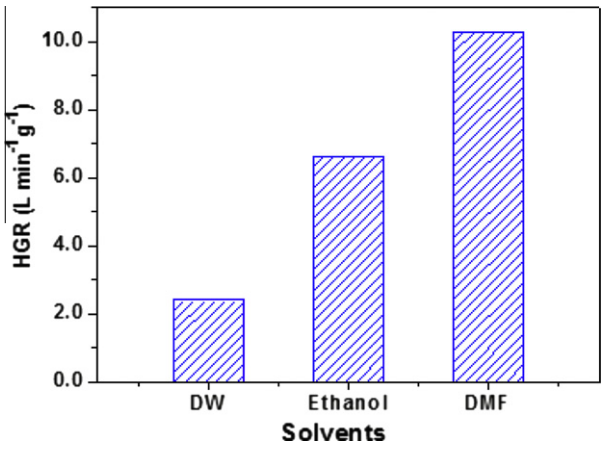

Fig. 3. Effects of the solvents used for preparation of the carbon-supported cobalt catalysts on their catalytic hydrogen generation activity by hydrolysis of 1 wt% $NaBH_4$ solution containing 8 wt% NaOH at 27 °C.

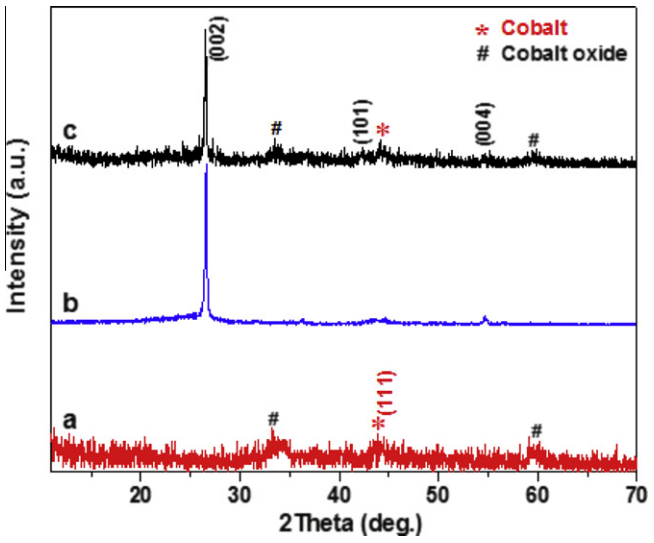

Fig. 4. XRD patterns of the unsupported cobalt particles (a), the carbon support (b), and the carbon-supported Co catalysts with the Co loading of 13.20 wt% which was synthesized under the optimum conditions (c).

comparing Fig. 4(c) with Fig. 4 (b) and (a) we can see that the diffraction peaks of (002), (101), and (004) in Fig. 4(c) are ascribable to the carbon support, and the rest peaks are very similar to those in the XRD pattern of the unsupported cobalt particles, implying that the carbon-supported cobalt catalyst has been successfully prepared.

Fig. 5 shows the typical SEM image of the carbon-supported cobalt catalyst prepared under the optimum conditions. It can be seen that the catalyst is comprised of irregular particles. The corresponding element composition and distribution are analyzed by EDS mapping, as shown in Fig. 5(b)–(d). These results indicate that the obtained catalyst consists of C, Co and O, which distribute very uniformly on the surface of carbon. The signal of oxygen originates from the oxidation products of both the carbon-support and the deposited cobalt, in accord with the analyses of FTIR and XRD aforementioned. The Co loading in the catalyst is determined to be 13.20 wt%. It is also found that increase of the Co loading in the range of 13.20–19.34 wt% does not change the particle-like morphology of the products.

TEM observation can provide more information about the microstructure of the catalyst. From the typical TEM images depicted in Fig. 6 we can clearly see that numerous sphere-like cobalt nanoparticles were uniformly deposited on the surface of the carbon support, in good agreement with the result of EDS mapping. The dimension of the ball-milled carbon is at micrometer scale, while the average diameter of the cobalt nanoparticles is about 15 nm. This fine microstructure is favorable for catalysis applications, which will be the focus of the succeeding parts.

3.3. Catalytic performance of the carbon-supported cobalt catalyst

3.3.1. Effect of Co loading

The effect of Co loading on the catalytic activity was evaluated by hydrolysis of 1 wt% $NaBH_4$ solution containing 8 wt% NaOH at 27 °C in the presence of 20 mg the carbon-supported cobalt nanoparticles with different Co loading. Fig. 7 displays the accumulated hydrogen volume as a function of time in the initial $NaBH_4$ hydrolysis process. For all the tested catalysts, the volume of generated hydrogen is almost proportional to the reaction time, indicating the stable catalytic activity of the catalysts. The H_2 yield, HGR and TOF for the catalysts with different Co loadings are tabulated in Table 1. It is clear that the catalytic activity of the catalyst increases with the Co loading, because higher Co loading leads to more active catalytic sites. This means that the hydrogen generation rate can be readily controlled by adjusting the Co loading.

3.3.2. Effect of catalyst dosage

The effect of catalyst dosage on the hydrogen generation is shown in Fig. 8, and the corresponding HGR normalized by the weight of cobalt and TOF are listed in Table 2. As expected, the HGR and TOF increase slightly with the amount of the cobalt catalyst used. This means that the hydrogen generation can also be controlled by tuning the dosage of the catalyst. From the inset of Fig. 8 we can see that the plot of ln(HGR) *vs* $\ln(m_{cobalt})$ is a straight line with a slope of 0.16. Therefore, the reaction order of the $NaBH_4$ hydrolysis catalyzed by the carbon-supported cobalt nanoparticles is 0.16 with respect to the concentration of cobalt. Possibly, the more the carbon-supported catalyst used, the more water molecules in the $NaBH_4$ solution were adsorbed, indirectly leading to the slight increase of $NaBH_4$ concentration and more contact between $NaBH_4$ and cobalt nanoparticles.

Hydrogen generation performance from $NaBH_4$ catalytic Hydrolysis is not only dependent on the catalytic activity of the catalyst used, but also on the hydrolysis conditions such as the concentration of both NaOH and $NaBH_4$, and the hydrolysis temperature [27]. Below we will discuss the effect of these outer conditions on the hydrolysis of $NaBH_4$ solution catalyzed by 20 mg of the milled-carbon-supported cobalt catalysts with a Co loading of 13.20 wt%.

3.3.3. Effect of NaOH concentration

NaOH is usually added as a stabilizer into the $NaBH_4$ solution to prevent its self-hydrolysis. Fig. 9 demonstrates the real-time hydrogen generation from $NaBH_4$ hydrolysis by changing the initial NaOH concentration in the range of 1–15 wt%. With increasing NaOH concentration from 1 to 10 wt%, the average HGR rises from 6.616 to 11.402 L_{H_2} min^{-1} g^{-1}_{cobalt}. However, further increase in the NaOH leads to a gradual decrease of the HGR due to the inhibition function of OH-with high concentration towards the hydrolysis reaction. Similar case was also reported for the colloidal carbon supported Co nanoparticles [27] and the activated carbon-supported Co–B catalysts catalyzed $NaBH_4$ hydrolysis reaction [28].

The quantitative relationship between the HGR and the NaOH concentration in the range of 1–10 wt% is given in the inset of Fig. 9. The plot of ln(HGR) *vs* $\ln(C_{NaOH})$ is a straight line with a slop of 0.23, suggesting that the reaction order is 0.23 with respect to the NaOH concentration. Herein, the increase of the NaOH

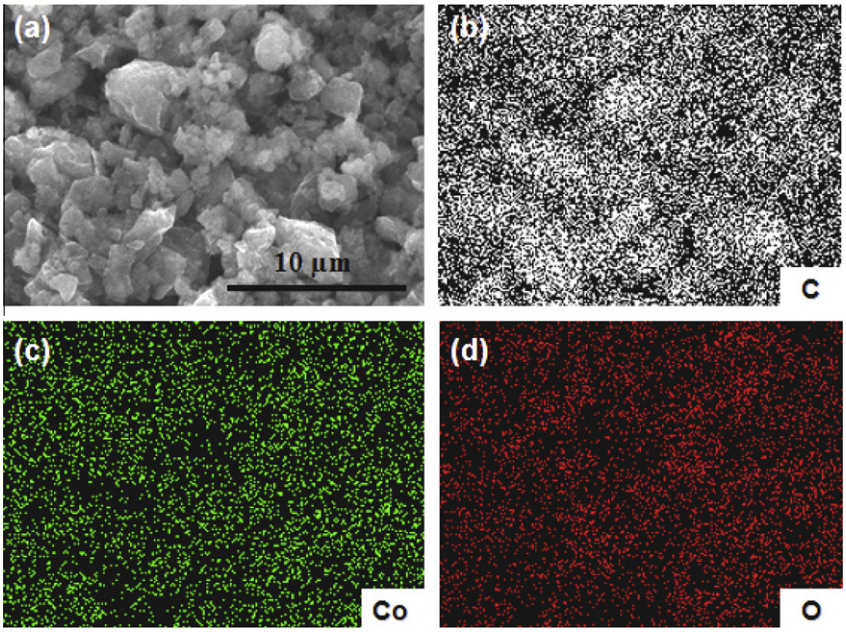

Fig. 5. A typical SEM image (a) of the carbon supported cobalt catalyst along with the corresponding EDS mapping of the constituent element C (b), Co (c), and O (d).

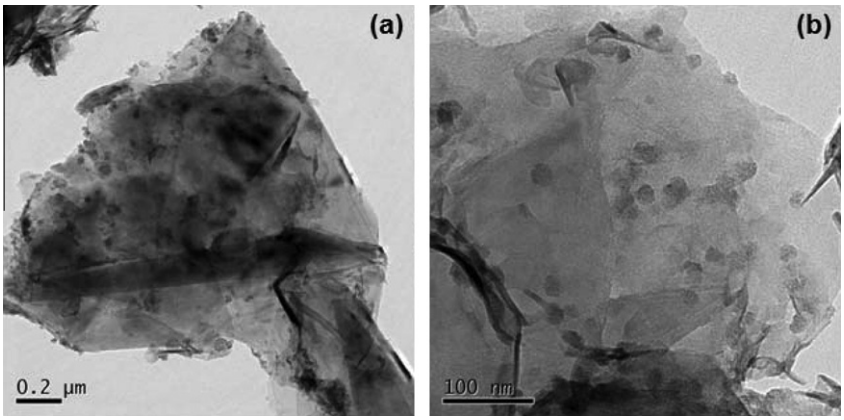

Fig. 6. Typical TEM images under different magnifications of the cobalt nanoparticles supported on the surface of the ball-milled carbon.

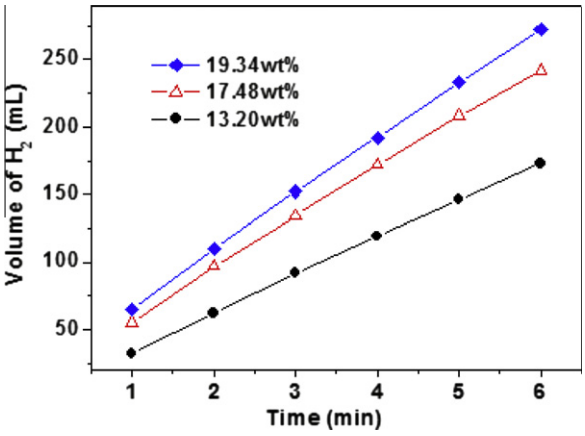

Fig. 7. Volume of the evolved H_2 as a function of time obtained by catalytic hydrolysis of 1 wt% $NaBH_4$ solution containing 8 wt% NaOH and 20 mg carbon-supported cobalt catalyst at 27 °C.

concentration in the range of 1–10 wt% has positive effect on the hydrogen generation. Possibly, an appropriate concentration of

Table 1
The effect of Co loading on the hydrogen generation performance.

Co loading (wt%)	13.20	17.48	19.34
H_2 Yield (%)	57	79	89
HGR ($L_{H_2} g^{-1}_{cobalt}$ min^{-1})	10.92	11.54	11.72
TOF (mol H_2 (mol Co)$^{-1}$ h^{-1})	1563.8	1651.9	1678.1

OH^- is beneficial to disperse the milled-carbon supported cobalt catalyst which carried a large quantity of oxygen-containing functional groups as discussed before, resulting in good contact between the catalyst and the $NaBH_4$ solution.

3.3.4. Effect of $NaBH_4$ concentration

Fig. 10 depicts the effect of the initial $NaBH_4$ concentration on the hydrogen generation performance. As can be seen from Fig. 10 that the hydrogen generation rate slightly increases with the $NaBH_4$ concentration ranging from 0.25 to 1.00 wt%, while gradually deceases with further increase of the $NaBH_4$ concentration. Theoretically, higher $NaBH_4$ concentration leads to higher

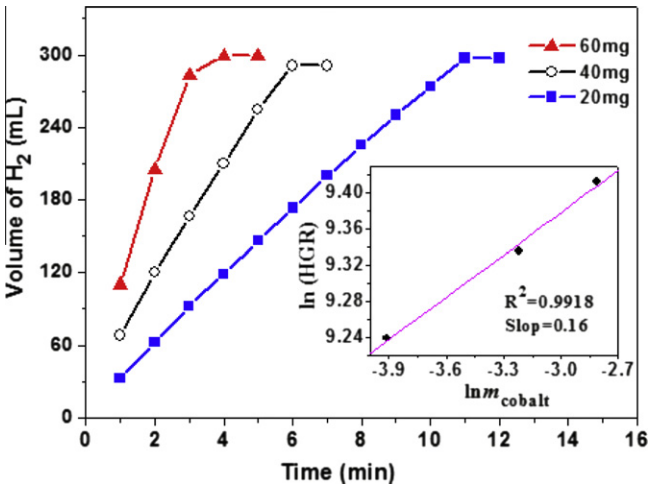

Fig. 8. Hydrogen generation as a function of reaction time obtained by hydrolysis of 1 wt% $NaBH_4$ solution containing 8 wt% NaOH and different amount of catalyst with the same Co loading of 13.20 wt% at 27 °C. The inset is the plot of the hydrogen generation rate (HGR) as a function of cobalt concentration (m_{cobalt}), both in logarithmic scale.

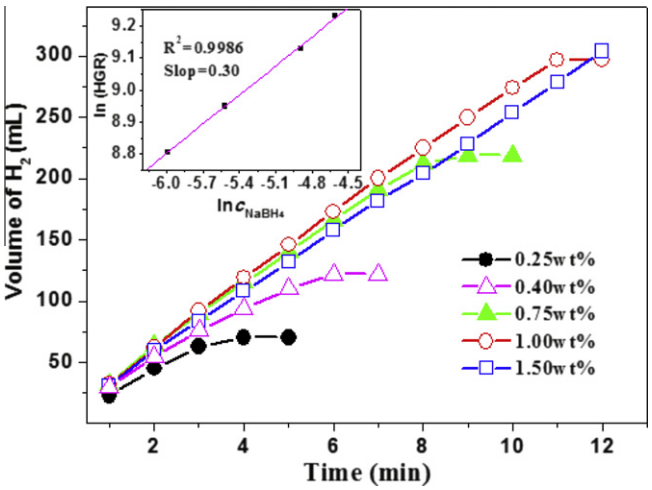

Fig. 10. Real-time hydrogen generation at 27 °C from the $NaBH_4$ solution of different concentration, which contains 8 wt% NaOH and 20 mg the carbon-supported cobalt catalyst with the Co loading of 13.20 wt%. The inset is the plot of ln(HGR) *vs* ln C_{NaBH_4}.

Table 2
The effect of catalyst dosage on the hydrogen generation performance.

Catalyst dosage (mg)	20	40	60
HGR ($L_{H_2}\,g_{cobalt}^{-1}\,min^{-1}$)	10.29	11.33	12.25
TOF (mol H_2 (mol Co)$^{-1}$ h^{-1})	1473.4	1622.2	1753.9

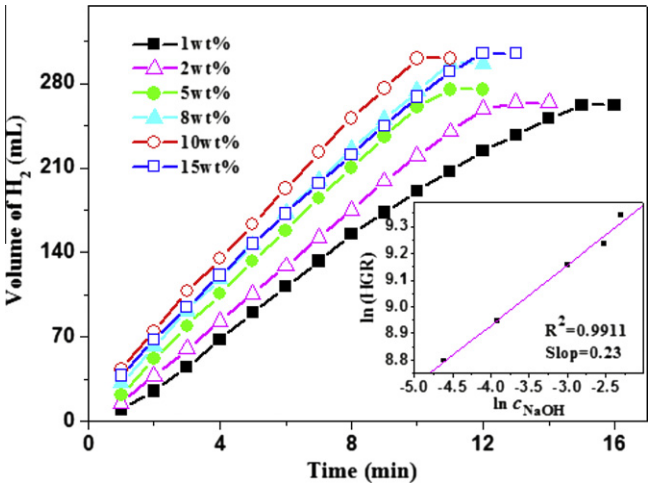

Fig. 9. Real-time hydrogen generation from the hydrolysis of 1 wt% $NaBH_4$ solution containing different concentration of NaOH at 27 °C in the presence of 20 mg the carbon-supported cobalt catalyst with the Co loading of 13.20 wt%. The inset is the plot of ln(HGR) *vs* ln(C_{NaOH}).

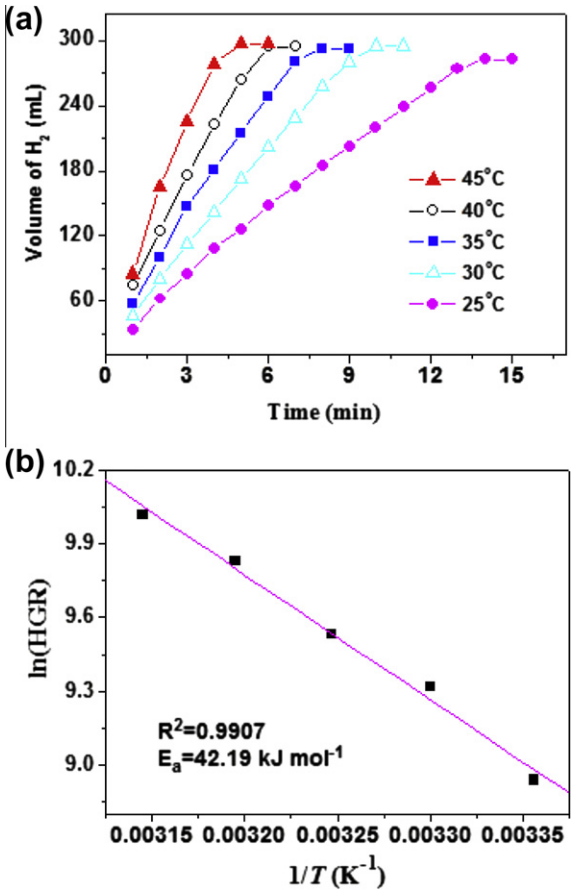

Fig. 11. (a) Real-time hydrogen generation from the 1 wt% $NaBH_4$ solution containing 8 wt% NaOH and 20 mg the carbon-supported cobalt catalyst with a Co loading of 13.20 wt% at different hydrolysis temperatures. (b) The Arrhenius plot of ln (HGR) *vs* 1/*T*.

hydrogen density. However, the alkalinity and viscosity of the hydrolysis system also increase with the $NaBH_4$ concentration, which prevents hydrogen generation and leads to a decrease of the HGR [29]. Similar case was also observed by Xu et al. in the $NaBH_4$ hydrolysis system using the cobalt catalysts supported by the modified activated carbon with concentrated HNO_3 oxidization [30].

The plot of ln(HGR) *vs* ln C_{NaBH_4} by fitting the points shown in the inset of Fig. 10 leads to a straight line with a slop of 0.30, implying that the reaction order is 0.30 with respect to the $NaBH_4$ concentration in the range of 0.25–1 wt%. Patel et al. found that the kinetics of $NaBH_4$ hydrolysis catalyzed by Co–P–B is dependent on the concentration of $NaBH_4$ [31]. For example, a first order kinetics was observed when the $NaBH_4$ concentration changed in the range of 0.005 to 0.05 M, while a near-zero kinetics was obtained in the range of 0.075–0.25 M. On the other hand, Zou

Table 3
The effect of hydrolysis temperature on the hydrogen generation performance.

Hydrolysis temperature (°C)	25	30	35	40	45
HGR ($L_{H_2}\,g^{-1}_{cobalt}\,min^{-1}$)	7.63	11.17	13.83	18.56	22.50
TOF (mol H_2 (mol Co)$^{-1}$ h^{-1})	1092.5	1599.3	1980.2	2657.4	3221.5

Table 4
Comparison of the key parameters for the $NaBH_4$ hydrolysis reaction catalyzed by different catalysts.

Catalysts	Activation energy (kJ mol^{-1})	H_2 generation rate ($L_{H_2}\,min^{-1}\,g^{-1}_{met}$)	Hydrolysis temperature (°C)	Ref.
Ru nanoclusters	28.51	3.65	25	[13]
Zeolite framework/Ni	60.4 ± 3.1	–	25	[14]
Vulcan XC-72/Co–B	57.8	2.3	25	[18]
MWCNT/Co–B	40.40	5.1	30	[19]
Carbon film/Co–B	~31	8.1	25	[20]
Active carbon/Co	45.64	0.07	30	[29]
γ-Al_2O_3/Co	32.63	0.22	30	[29]
AMPS hydrogels/Co	38.14	0.94	30	[33]
hydroxyapatite/Co	53 ± 2	5.0	25	[35]
Co–Cu–B	49.6	4.8	30	[36]
$LiCoO_2$/Ru	68.5	3.0	25	[37]
$LiCoO_2$/Pt	70.4	2.7	25	[37]
IR-120/Ru	49.72	0.132	25	[38]
Ni–Ru	52.73	0.4	35	[39]
Attapulgite clay/Co–B	56.32	1.27	25	[40]
Pd–TiO_2–P/Co–Ni	57.0	0.46	25	[41]
Co–Mn–B	52.1	2.5	30	[42]
Ni–Fe–B	57	2.91	25	[43]
PVP-stabilized Co(0)	37 ± 2	9.36	25	[44]
Intrazeolite/Co	34 ± 2	6.09	25	[45]
PEG-stabilized Fe(0)	37.0 ± 2.0	–	25	[46]
Zeolite/Ru nanoclusters	34.9 ± 2.0	14.7	25	[47]
Ni foam/Co–W–B	29	15	30	[48]
Modified carbon/Co	42.19	10.29	27	This work

et al. reported the reaction order with regard to $NaBH_4$ is −0.25 and 0.27, respectively, for the powder-like and spherical Ru/C catalysts [32]. Sahiner et al. found that the hydrolysis reaction of $NaBH_4$ with p(AMPS)-Co composite catalyst system is zero order with respect to initial concentration of $NaBH_4$ [33]. Shang et al. reported that the hydrolysis $NaBH_4$ over ruthenium catalyst is zero order to $NaBH_4$ concentration when water is sufficient [34]. Accordingly, the kinetics of $NaBH_4$ hydrolysis is not only dependent on its concentration range, but also on the type of the catalysts used for hydrogen generation. Further investigations should be performed to better understand the effects of the $NaBH_4$ concentration on the mechanisms involved in the hydrolysis process.

3.3.5. Effect of hydrolysis temperature

Fig. 11(a) presents the effect of hydrolysis temperature on the hydrogen generation performance of the $NaBH_4$ hydrolysis reaction. As can be seen from the slope of the linear portion and the hydrolysis duration time that hydrogen generation rate increase with the reaction temperature. The corresponding average HGR as well as the corresponding TOF at each temperature is listed in Table 3, indicating that the hydrolysis rate can also be controlled by adjusting the reaction temperature.

The average HGR data in Table 3 are further used to determine the activation energy for the $NaBH_4$ hydrolysis catalyzed by the carbon-supported cobalt nanoparticles according to the Arrhenius equation:

$$\ln(\mathrm{HGR}) = \ln A - \frac{E_a}{RT} \quad (1)$$

where HGR is the average hydrogen generation rate ($L_{H_2}\,min^{-1}\,g^{-1}_{cobalt}$), A is the pre-exponential factor, E_a is the activation energy (kJ mol^{-1}), R is the gas constant (8.314 J mol^{-1} K^{-1}), and T is the hydrolysis temperature (K). The Arrhenius plot of ln(HGR) *vs* ln(1/T) is shown in Fig. 11(b). The slope of the straight line gives the activation energy of 42.19 kJ mol^{-1}, which is lower than most of the reported data as summarized in Table 4.

On the basis of the above discussion about the influence factors of the hydrogen generation, the final rate equation for the carbon-supported cobalt nanoparticles catalyzed $NaBH_4$ hydrolysis reaction is described as:

$$r = A\exp(-42190/RT)[\mathrm{cobalt}]^{0.16}[\mathrm{NaOH}]^{0.23}[\mathrm{NaBH_4}]^{0.30} \quad (2)$$

4. Conclusion

The catalytic hydrogen generation activity of the carbon-supported cobalt catalysts toward $NaBH_4$ hydrolysis reaction was significantly improved by ball-milling pretreatment of the carbon support and screening the solvents used for preparing the catalysts. The high performance of the modified carbon-supported cobalt catalyst is supported by its low activation energy (42.19 kJ mol^{-1}) and high average hydrogen generation rate (10.29 L_{H_2} min^{-1} g^{-1}_{cobalt}).

Acknowledgements

This work was financially supported by the National Natural Science Foundation of China (51071131), Program for New Century Excellent Talents in University (NCET-10-0890), and the Scientific Research Foundation for the Returned Overseas Chinese Scholars ([2008]488).

References

[1] M.Z. Jacobson, W.G. Colella, D.M. Golden, Science 308 (2005) 1901–1905.
[2] P. Chen, M. Zhu, Mater. Today 11 (2008) 36–43.
[3] I.P. Jain, P. Jain, A. Jain, J. Alloys compd. 503 (2010) 303–339.
[4] J. Yang, A. Sudik, C. Wolverton, D.J. Siegel, Chem. Soc. Rev. 39 (2010) 656–675.
[5] C. Liang, Y.F. Liu, H. Fu, Y. Ding, M. Gao, H.G. Pan, J. Alloys compd. 509 (2011) 7844–7853.
[6] D.M.F. Santos, C.A.C. Sequeira, Renew. Sust. Energ. Rev. 15 (2011) 3980–4001.
[7] B. Sakintuna, F. Lamari-Darkrim, M. Hirscher, Int. J. Hydrogen Energy 32 (2007) 1140–1211.
[8] S. Orimo, Y. Nakamori, J.R. Eliseo, A. Züttel, C.M. Jensen, Chem. Rev. 107 (2007) 1140–1211.
[9] B.H. Liu, Z.P. Li, J. Power Source 187 (2009) 527–534.
[10] U.B. Demirci, O. Akdim, J. Andrieux, J. Hannauer, R. Chamoun, P. Miele, Fuel Cells 10 (2010) 335–350.
[11] S.S. Muir, X. Yao, Int. J. Hydrogen Energy 36 (2011) 5983–5997.
[12] B.H. Liu, Z.P. Li, S. Suda, J. Alloys Compd. 415 (2006) 288–293.
[13] S. Özkar, M. Zahmakıran, J. Alloys Compd. 404–406 (2005) 728–731.
[14] M. Zahmakıran, T. Ayvalı, S. Akbayrak, S. Çalışkan, D. Çelik, S. Özkar, Catal. Today 170 (2011) 76–84.
[15] D. Xu, P. Dai, X. Liu, C. Cao, Q. Guo, J. Power Sources 182 (2008) 616–620.
[16] S.U. Jeong, E.A. Cho, S.W. Nam, I.H. Oh, U.H. Jung, S.H. Kim, Int. J. Hydrogen Energy 32 (2007) 1749–1754.
[17] B.H. Liu, Q. Li, Int. J. Hydrogen Energy 33 (2008) 7385–7391.
[18] J. Zhao, H. Ma, J. Chen, Int. J. Hydrogen Energy 32 (2007) 4711–4716.
[19] Y. Huang, Y. Wang, R. Zhao, P. Shen, Z. Wei, Int. J. Hydrogen Energy 33 (2008) 7110–7115.
[20] N. Patel, R. Fernandes, N. Bazzanella, A. Miotello, Catal. Today 170 (2011) 20–26.
[21] L. Gao, C. Chen, L. Chen, Q. Wang, C. Wang, Y. An, J. Alloys Compd. 424 (2006) 338–341.
[22] S. Liu, L. Sun, Y. Zhang, F. Xu, J. Zhang, H. Chu, M. Fan, T. Zhang, X. Song, J.P. Grolier, Int. J. Hydrogen Energy 34 (2009) 8079–8085.
[23] C. Liu, Y. Kuo, B. Chen, C. Hsueh, K. Hwang, J. Ku, F. Tsau, M. Jeng, Int. J. Hydrogen Energy 35 (2010) 4027–4040.
[24] A.W. Heinen, J.A. Peters, H. Bekkum, Appl. Catal. A 194–195 (2000) 193–202.
[25] J.P. Chen, S. Wu, Langmuir 20 (2004) 2233–2242.
[26] U.B. Demirci, P. Miele, Phys. Chem. Chem. Phys. 12 (2010) 14651–14665.
[27] J. Zhu, R. Li, W. Niu, Y. Wu, X.L. Gou, J. Power Source 211 (2012) 33–39.
[28] D. Xu, H. Wang, Q. Guo, S. Ji, Fuel Process. Technol. 92 (2011) 1606–1610.
[29] W. Ye, H. Zhang, D. Xu, L. Ma, B. Yi, J. Power Sources 164 (2007) 544–548.
[30] D. Xu, P. Dai, Q. Guo, X. Yue, Int. J. Hydrogen Energy 33 (2008) 7371–7377.
[31] N. Patel, R. Fernandes, A. Miotello, J. Power Source 188 (2009) 411–420.
[32] Y.C. Zou, M. Nie, Y.M. Huang, J.Q. Wang, H.L. Liu, Int. J. Hydrogen Energy 36 (2011) 12343–12351.
[33] N. Sahiner, O. Ozay, E. Inger, N. Aktas, Appl. Catal. B 102 (2011) 201–206.
[34] Y. Shang, R. Chen, G. Jiang, Int. J. Hydrogen Energy 33 (2008) 6719–6726.
[35] M. Rakap, S. Özkar, Catal. Today 183 (2012) 17–25.
[36] X. Ding, X. Yuan, C. Jia, Z. Ma, Int. J. Hydrogen Energy 35 (2010) 11077–11084.
[37] Z. Liu, B. Guo, S.H. Chan, E.H. Tang, L. Hong, J. Power Source 176 (2008) 306–311.
[38] C. Hsueh, C. Chen, J. Ku, S. Tsai, Y. Hsu, F. Tsau, M. Jeng, J. Power Sources 177 (2008) 485–492.
[39] C. Liu, B. Chen, C. Hsueh, J. Ku, M. Jeng, F. Tsau, Int. J. Hydrogen Energy 34 (2009) 2153–2163.
[40] H. Tian, Q. Guo, D. Xu, J. Power Sources 195 (2010) 2136–2142.
[41] M. Rakap, E.E. Kalu, S. Özkar, J. Alloys Compd. 509 (2011) 7016–7021.
[42] X. Yuan, C. Jia, X. Ding, Z. Ma, Int. J. Hydrogen Energy 37 (2012) 995–1001.
[43] M. Nie, Y.C. Zou, Y.M. Huang, J.Q. Wang, Int. J. Hydrogen Energy 37 (2012) 1568–1576.
[44] Ö. Metin, S. Özkar, Energy Fuel 23 (2009) 3517–3526.
[45] M. Rakap, S. Özkar, Appl. Catal. B 91 (2009) 21–29.
[46] M. Dinç, Ö. Metin, S. Özkar, Catal. Today 183 (2012) 10–16.
[47] M. Zahmakiran, S. Özkar, Langmuir 25 (2009) 2667–2678.
[48] H.B. Dai, Y. Liang, P. Wang, X.D. Yao, T. Rufford, M. Lu, H.M. Cheng, Int. J. Hydrogen Energy 33 (2008) 4405–4412.